

# Optical Properties of Thermally Evaporated $\text{Bi}_2\text{Te}_{3x}\text{Se}_{3(1-x)}$ Thin Films for Optoelectronic Applications

G. D. Deshmukh

Associate Professor, Department of Physics

Nanasaheb Y. N. Chavan Arts, Science and Commerce College, Chalisgaon, Dist. Jalgaon, India

**Abstract:** This study investigates the optical properties of thermally evaporated bismuth telluride-selenide ( $\text{Bi}_2\text{Te}_{3x}\text{Se}_{3(1-x)}$ ) thin films with varying selenium content. The films were deposited on glass substrates using thermal evaporation technique under high vacuum conditions. Optical characterization was performed through UV-Visible-NIR spectrophotometry to determine transmission, reflection, absorption coefficient, refractive index, extinction coefficient, and optical band gap. For all the films, transmittance spectra reveal very pronounced interference effects for wavelength away from the fundamental absorption edge. With increasing the composition of  $\text{Bi}_2\text{Te}_3$  ( $x = 0$  to 0.9) the absorption edge shifts towards lower wavelength region. The optical band gap has been found to be direct and allowed, it increases from 0.62 to 0.82 with increase in composition from  $x = 0.1$  to 0.9. The value of extinction coefficient 'k' varies between 0.36 and 1.48, while refractive index 'n' varies between 1.48 and 7.64, for all the compositions. The number of well-defined turning points is observed in variations of optical constants n and k with  $\lambda$ .

**Keywords:**  $\text{Bi}_2\text{Te}_{3x}\text{Se}_{3(1-x)}$ , thermal evaporation, optical properties, thin films, band gap, refractive index

## I. INTRODUCTION

Thin film technology has emerged as a pivotal area of research, offering versatile applications across optoelectronics, thermoelectrics, and energy conversion systems [1]. Among the diverse materials explored for these applications, chalcogenide thin films, particularly those based on bismuth telluride and selenium  $\text{Bi}_2\text{Te}_{3x}\text{Se}_{3(1-x)}$ , exhibit fascinating optical properties crucial for device development [2]. The tunable stoichiometry of  $\text{Bi}_2\text{Te}_{3x}\text{Se}_{3(1-x)}$  alloys allows for systematic manipulation of their electronic band structure, consequently influencing their optical absorption, reflectivity, and transmittance spectra [3]. This tunability is particularly significant for applications requiring specific band gap energies, such as photodetectors and solar cells, where precise control over light absorption characteristics is paramount. Furthermore, the exploration of direct band-edge transitions in these materials is vital for optimizing their performance in luminescence and solar energy devices [4]. The accurate determination of optical constants like refractive index, extinction coefficient, and absorption coefficient is critical for predicting the applicability and performance of these thin films in advanced photonic technologies [5]. This paper delves into the optical properties of thermally evaporated  $\text{Bi}_2\text{Te}_{3x}\text{Se}_{3(1-x)}$  thin films, investigating the impact of varying selenium concentrations on their fundamental optical parameters and electronic transitions. Such investigations are crucial for advancing the design and fabrication of high-performance optoelectronic devices, leveraging the unique characteristics of chalcogenide semiconductors [6].

## II. EXPERIMENTAL

**Deposition of  $\text{Bi}_2\text{Te}_{3x}\text{Se}_{3(1-x)}$  films:** By means of  $\text{Bi}_2\text{Te}_3$  and  $\text{Bi}_2\text{Se}_3$  powder (Sigma-Aldrich 99.99+ % purity) the ternary thin films of  $\text{Bi}_2\text{Te}_{3x}\text{Se}_{3(1-x)}$  ( $x = 0.1$  to 0.9) were deposited by means of sublimation of the compound onto well cleaned glass substrates by thermal evaporation in vacuum ( $\approx 10^{-5}$  torr) with molybdenum boat as a source. So as to prepare ternary semiconductors of  $\text{Bi}_2\text{Te}_{3x}\text{Se}_{3(1-x)}$  ( $x = 0.1$  to 0.9) the constituent compounds of  $\text{Bi}_2\text{Te}_3$  and  $\text{Bi}_2\text{Se}_3$  have been taken in molecular stoichiometry proportional weights, crushed and mixed homogenously. The diverse sets of samples of varying compositions ( $x = 0.1$  to 0.9) with different thicknesses for the ternaries were deposited under precise growth conditions.

Copyright to IJARSCT

[www.ijarsct.co.in](http://www.ijarsct.co.in)

The rate of deposition and thickness of the films were organized by using quartz crystal thickness monitor model no. DTM-101 provided by HINDHIVAC. The deposition rate was maintained 3–5 Å/sec constant during the course of the sample preparations. The film thicknesses were long-established by using weight-difference method with the help of digital balance (DENOVER- Model: TB-214, Germany) having accuracy of 0.1mg. The source to substrate distance was kept constant (14 cm). The alumel-chromel thermocouple placed in contact with the substrates continuously records the substrate temperature ( $\approx 306$  K). The selected samples of  $\text{Bi}_2\text{Te}_{3x}\text{Se}_{3(1-x)}$  ( $x = 0.1$  to  $0.9$ ) thin films having closely equal thicknesses ( $\approx 2500$  Å) were used for the study. These samples were annealed at 423 K for 30 min. in vacuum ( $\approx 10^{-5}$  torr) and used for the characterization.

**Structural Characterization:** The X-ray diffraction (XRD) patterns of selected  $\text{Bi}_2\text{Te}_{3x}\text{Se}_{3(1-x)}$  annealed samples were recorded by X-ray diffractometer (Bruker, model D-8 Advance) with  $\text{CuK}\alpha$  radiation (1.5406 Å). The surface morphology and the chemical composition of these films were investigated by field emission scanning electron microscope (FESEM) attached with EDAX using model Hitachi S-4800-II (Japan). The film micrographs are also studied using transmission electron microscope (TEM) and selected area electron diffraction (SAD) via model FEI TECNAI-G<sup>2</sup>.

**Optical measurement:** The transmittance  $T(\lambda)$  and reflectance  $R(\lambda)$  of the films were measured in the spectral range of 200–2500 nm, using the model JASCO V-670 UV–VIS–NIR double beam spectrophotometer. The absorption coefficient ( $\alpha$ ), atomic spacing ( $d$ ), grain size ( $D$ ), microstrain ( $\epsilon$ ), dislocation density ( $\delta$ ), lattice parameter ( $a$ ), types of transition, optical constants ( $n$  and  $k$ ) and optical band gap ( $E_g$ ) were determined from these studies for annealed  $\text{Bi}_2\text{Te}_{3x}\text{Se}_{3(1-x)}$  thin film samples.

### III. RESULT AND DISCUSSION

**Structural analysis:** The X-ray diffraction patterns of the thermally evaporated  $\text{Bi}_2\text{Te}_{3x}\text{Se}_{3(1-x)}$  ( $x = 0.2, 0.4$  and  $0.6$ ) thin films of thickness 2500 Å annealed at 423 K for 30 min. in vacuum ( $\approx 10^{-5}$  torr) are shown in Fig.1.

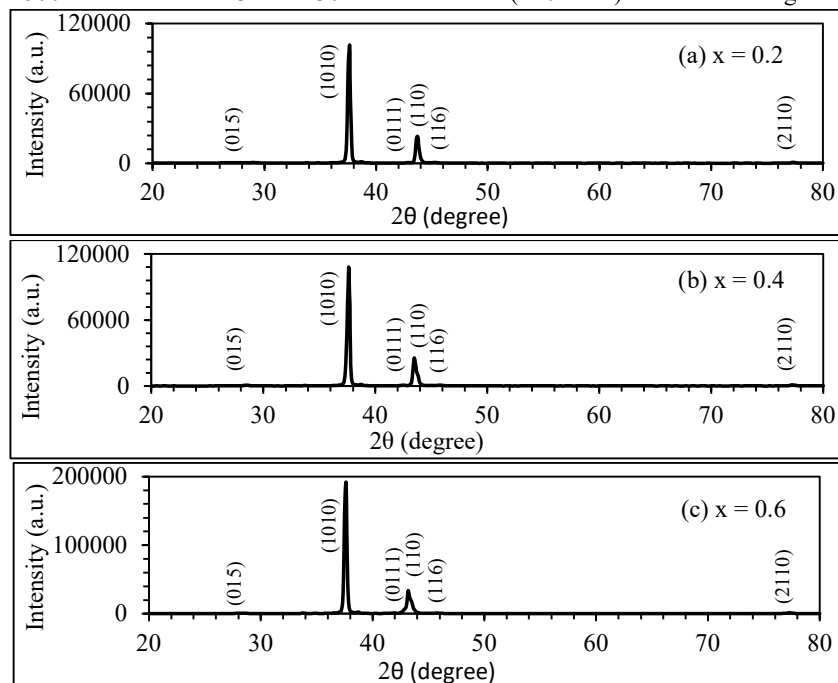


**Fig.1** XRD patterns of  $\text{Bi}_2\text{Te}_{3x}\text{Se}_{3(1-x)}$  thin films annealed at 423 K for 30 min in vacuum ( $\approx 10^{-5}$  torr)

The XRD patterns shows that, all the films are polycrystalline exhibiting rhombohedral structure which is usually represented in the hexagonal lattice, with strong preferential orientation of the crystallites along (1010) direction for all the compositions. These samples also show lower intensity peaks for (015), (0111), (116) and (2110) directions. It is observed that the intensity of peaks is maximum for the film with composition  $x = 0.7$ , while it is minimum for  $x = 0.3$ .

The intensity of peaks increases from composition  $x = 0.1$  to  $x = 0.7$  except  $x = 0.3$ , then it decreases up to  $x = 0.9$ . The experimental d-values for the different compositions of  $\text{Bi}_2\text{Te}_{3x}\text{Se}_{3(1-x)}$  ternary system are calculated using the Bragg's law for each composition along the prominent peak corresponding to (1010) rhombohedral structure and compared with the standard American Standard for Testing and Materials (ASTM) data card d-values ( $d^*$ ) obtained from Vegard's law for  $\text{Bi}_2\text{Te}_{3x}\text{Se}_{3(1-x)}$  system.

#### FESEM and TEM analysis:

The field emission scanning electron microscope images of  $\text{Bi}_2\text{Te}_{3x}\text{Se}_{3(1-x)}$  thin films of different compositions are shown in Fig. 2. The images show that the deposited films are having uniform deposition, homogeneous surface and are polycrystalline in nature. All films illustrate well adherent, uniform film surface without cracks and good crystallinity. The grain size observed from the FESEM images is about 25-50 nm.

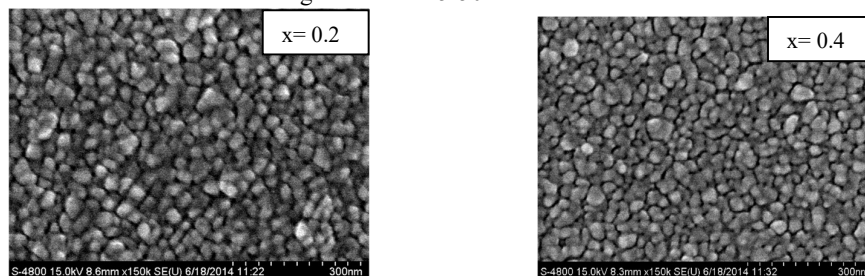


**Fig. 2** FESEM micrographs of thermally evaporated annealed  $\text{Bi}_2\text{Te}_{3x}\text{Se}_{3(1-x)}$  films of different compositions

The transmission electron microscope (TEM) images and electron diffraction patterns of  $\text{Bi}_2\text{Te}_{3x}\text{Se}_{3(1-x)}$  thin films for the composition  $x=0.9$  are shown in Fig. 3 (a) - (b). The electron micrographs also confirm the presence of fine crystallites in the film. The d-values obtained using electron diffraction pattern are comparable with the d-values of the thin film obtained using the XRD pattern.

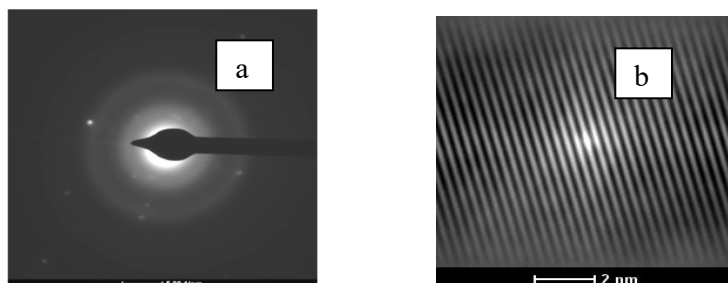


**Fig.3** TEM micrographs and electron diffraction patterns of thermally evaporated annealed  $\text{Bi}_2\text{Te}_{3x}\text{Se}_{3(1-x)}$  films for composition  $x=0.9$

**Optical analysis:** The optical transmittance and reflectance spectra of these  $\text{Bi}_2\text{Te}_{3x}\text{Se}_{3(1-x)}$  films, annealed at 423 K for 30 min. in vacuum ( $\approx 10^{-5}$  torr) were recorded using JASCO V-670 UV-VIS-NIR double beam spectrophotometer in the spectral range of 200–2500 nm and are shown in Fig. 4 and 5 respectively.

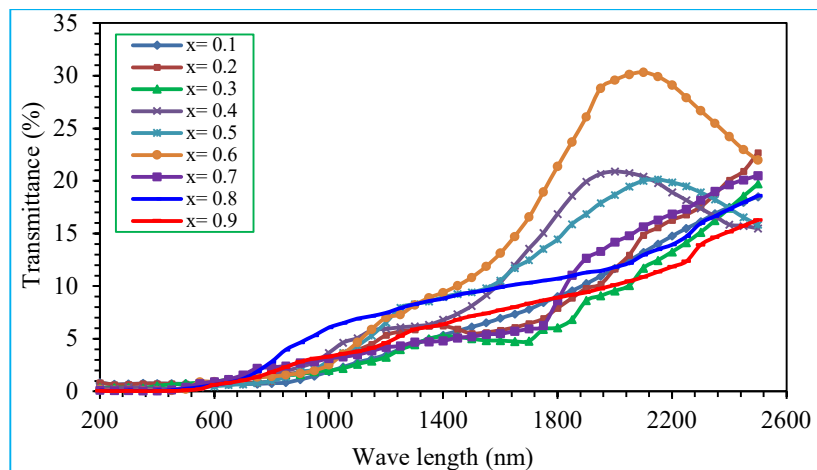


**Fig.4** Transmittance spectra of  $\text{Bi}_2\text{Te}_{3x}\text{Se}_{3(1-x)}$  thin films annealed at 423 K for 30 min. in vacuum

The occurrence of maxima and minima in the optical spectra ensure the optical homogeneity in the films. The optical transmission is a complex function and depends upon the refractive index of the substrate, refractive index of the film, film thickness and the wavelength of the incident light [7]. For all the films, spectra reveal very distinct interference effects for wavelength away from the fundamental absorption edge. High transmittance in a higher wavelength region and a sharp absorption edge were observed in the films.

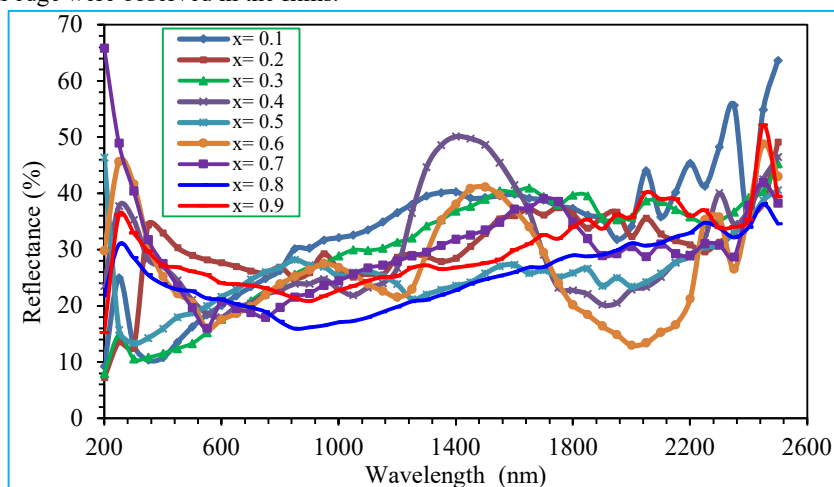


**Fig. 5** Reflectance spectra of  $\text{Bi}_2\text{Te}_{3x}\text{Se}_{3(1-x)}$  thin films annealed at 423 K for 30 min. in vacuum

The samples show optical transparency exhibiting interference pattern in the spectral region between 700 nm to 2500 nm and display a clear absorption edge interrelated to the optical band gap depending on the composition of the films. The film with composition  $x = 0.6$  shows maximum optical transparency 30 % at the wavelength 2000 nm. The remaining all compositions show optical transparency between 0-20% in the spectral range of 200-2500 nm. With the increase in  $x$  from 0.1 to 0.9 i.e. increasing the composition of  $\text{Bi}_2\text{Te}_3$  in to the film, the absorption edge shifts towards lower wavelength region. The transmittance falls steeply with decreasing wavelength. This disclose that the  $\text{Bi}_2\text{Te}_{3x}\text{Se}_{3(1-x)}$  films are having considerable absorption throughout the wavelength region 200–700 nm depending on the composition. The emergence of the maxima and minima results from the interference effect and their number depends on the thickness of the films. For all compositions this number of maxima and minima is seen to be nearly same. Such performance of the transmission spectra is the confirmation of the equal thickness and uniformity of the films. For all the films the reflectance lies between 10-60% in the spectral range of 200-2500 nm.

Absorption coefficients ( $\alpha$ ) have been evaluated using percentage transmittance data with following equation

$$\alpha = \frac{2.303}{d} \log_{10} \left( \frac{1}{T} \right) \quad (1)$$

Where  $d$  is the thickness and  $T$  is the transmittance of the film.

The absorption coefficient can be written in general form as a function of incident photon energy  $h\nu$  as

$$\alpha h\nu = A (h\nu - E_g)^P \quad (2)$$

Where  $E_g$  is the optical band gap,  $A$  is a constant and  $P$  has discrete values like  $1/2$ ,  $3/2$ ,  $2$  or more depending on whether the transition is direct or indirect, and allowed or forbidden. In the direct and allowed cases  $P = 1/2$ , whereas for the direct but forbidden cases it is  $3/2$ . But for the indirect and allowed case  $P = 2$  and for the forbidden cases it will be  $3$  or more. The value of  $P$  determines the nature of optical transition. The results have been examined according to relation (2). The plot of  $(\alpha h\nu)^2$  versus  $h\nu$  for these annealed films is presented in Fig 6 (a) to (i).

It was found that the optical band gap increases gradually from 0.62 eV to 0.82 eV with increase in Te concentration. Analogous results were reported by S. Augustine et al [8]. The closer value of band gap (0.6 eV) in favor of direct transition was determined by A. Zimmer et al [9] for the electroplated  $n\text{-Bi}_2(\text{Te}_{0.9}\text{Se}_{0.1})_3$  thin films. Tellurium doped thin films have got higher band gaps compared to the undoped  $\text{Bi}_2\text{Se}_3$  thin films. The reason is that selenium atoms are smaller than tellurium atoms and possess lower-energy atomic orbit, which can lead to wider energy gap by lowering top of the valence band and more importantly raising the bottom of conduction band [10].

Optical constants such as refractive indices ( $n$ ) and extinction coefficients ( $k$ ) have been evaluated from the transmittance and reflectance data and using the following relations for normal incidence [11].

$$R = \frac{[(n-1)^2 + k^2]}{[(n+1)^2 + k^2]} \quad (3)$$

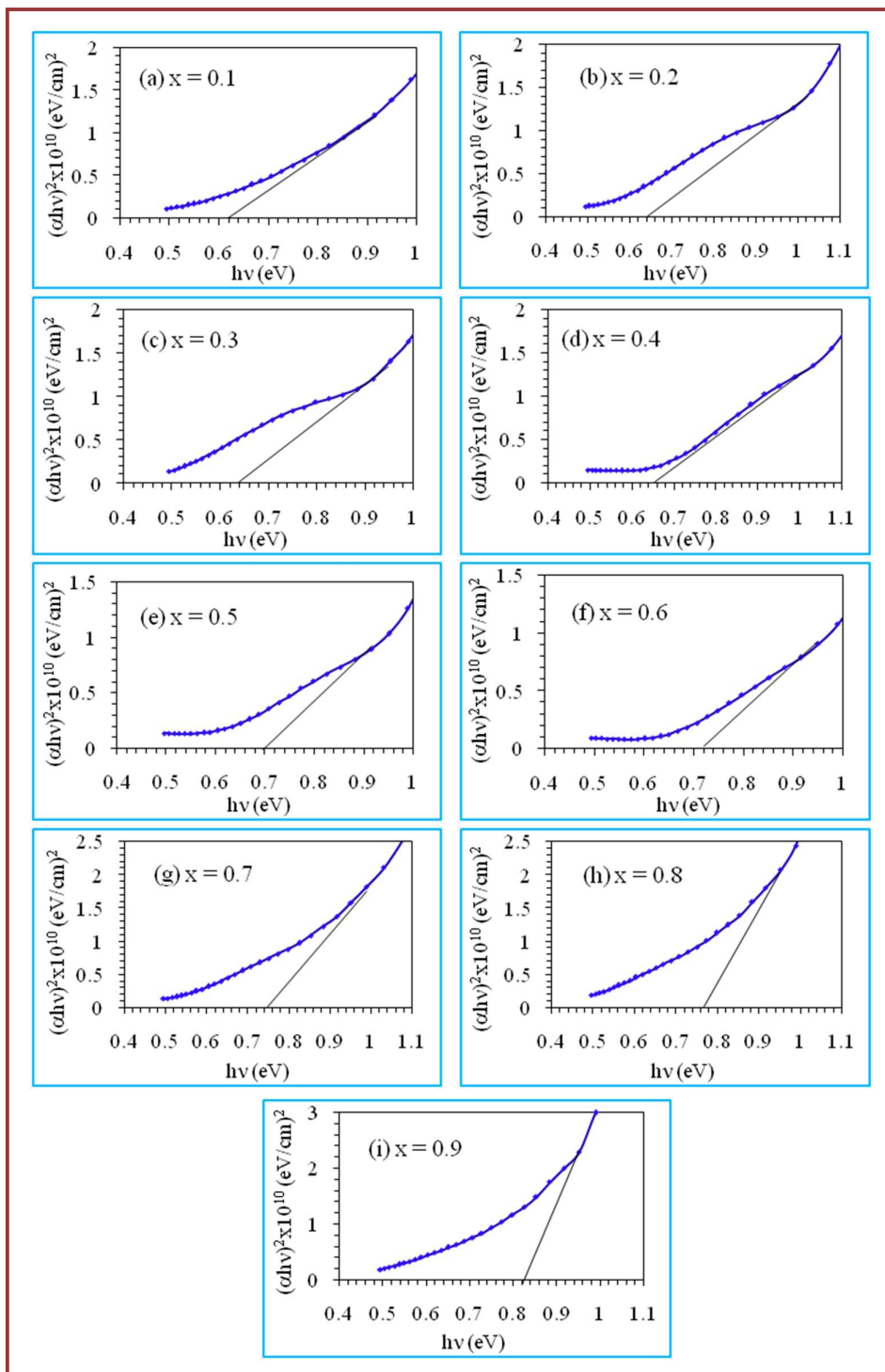
$$k = \frac{\alpha\lambda}{4\pi} \quad (4)$$

Table 1 represents variation of band gap ( $E_g$ ) with the composition ( $x$ ) and also the comparison of maxima and minima on the variation of  $n$  and  $k$  with wavelength for these  $\text{Bi}_2\text{Te}_{3x}\text{Se}_{3(1-x)}$  thin films.

From the Table 1 it is seen that variations of  $n$  and  $k$  are fairly oscillatory in nature. Also the number of well-defined turning points is observed i.e. number of maxima or minima are varying by changing the compositions of the films. The oscillatory behaviour is moderate for the compositions  $x = 0.5$  and  $0.7$ . The result shows an abrupt decrease of 'n' and increase of 'k' with  $\lambda$  over the spectral range from 200 to 500 nm after which it becomes oscillatory with increasing wavelength in the transparent region. For all compositions the extinction coefficient 'k' varies between 0.36 and 1.48, whereas refractive index 'n' varies between 1.48 and 7.64. The comparable ranges of values are reported by A. Kumar et al [7], S. Augustine et al [8] and P. B. Barman et al [12].

It is also observed that the value of refractive index show almost an overall increasing oscillatory trend with increase in wave length in the region 1800 to 2500 nm. This spectral and dopant dependence of optical constants with the wave length or photonic energy will be helpful in deciding on the suitability of this system for application in optical data storage devices [13]. The values of refractive indices ( $n$ ) and extinction coefficients or absorption indices ( $k$ ) obtained over the visible region of the spectrum are nearly invariable and independent of the composition.





**Fig. 6** Variation of  $(\alpha hv)^2$  with photon energy ( $h\nu$ ) for annealed  $\text{Bi}_2\text{Te}_x\text{Se}_{3(1-x)}$  thin films

**Table 1** Variation of band gap with the composition and the comparison of maxima and minima on the variation of n and k with wavelength for annealed  $\text{Bi}_2\text{Te}_{3x}\text{Se}_{3(1-x)}$  thin films in vacuum ( $\approx 10^{-5}$  torr).

Composition of the film (x)	Eg (eV)	Maxima			Minima		
		$\lambda$ (nm)	n	k	$\lambda$ (nm)	n	k
0.1	0.62	250	2.9	----	400	1.72	----
		900	----	1.29	1100	----	1.26
		1800	----	1.38	2350	----	1.33
		2350	5.34	----	2400	2.75	----
0.2	0.63	350	3.47	----	850	1.96	----
		950	----	1.21	1050	----	1.1
		1750	----	1.49	2100	----	1.27
		2050	2.84	----	2250	2.20	----
0.3	0.64	250	2.40	----	500	1.53	----
		1200	----	1.31	1250	----	1.28
		1550	3.20	----	1950	2.54	----
		1700	----	1.65	2000	----	1.49
0.4	0.66	250	3.78	----	600	1.64	----
		950	----	1.08	600	----	0.92
		1400	4.63	----	1900	1.75	----
		1500	----	1.20	1950	----	0.98
0.5	0.70	800	----	1.18	1250	----	1.01
		850	2.28	----	1250	1.79	----
		1550	----	1.15	2000	1.90	----
		1850	2.26	----	2050	----	1.07
0.6	0.72	250	4.48	----	550	----	0.81
		450	----	1.01	600	1.67	----
		950	----	1.19	1950	----	0.77
		1500	3.69	----	2000	1.51	----
0.7	0.74	450	----	0.94	550	----	0.86
		600	2.03	----	550	1.59	----
		1750	----	1.54	2000	----	1.24
		2450	3.62	----	2350	2.16	----
0.8	0.76	250	3.12	----	850	----	0.87
		450	----	0.99	850	1.48	----
		2250	----	1.38	2250	----	1.37
		2450	3.12	----	2350	2.41	----
0.9	0.82	250	3.51	----	600	----	0.97
		450	----	1.12	900	1.62	----
		2250	----	1.50	2300	----	1.44
		2450	4.75	----	2350	2.47	----

#### IV. CONCLUSIONS

The X-ray diffraction of thermally evaporated  $\text{Bi}_2\text{Te}_{3-x}\text{Se}_{3(1-x)}$  thin films indicates that, for all the compositions films are polycrystalline exhibiting rhombohedral structure represented in the hexagonal lattice strongly orientated along (1010) direction. The grain size observed from the FESEM images are about 25-50 nm. The TEM images confirm the presence of fine crystallites in the film. The d-values obtained using electron diffraction pattern and using the XRD are comparable. For all the films, transmittance spectra reveal very pronounced interference effects for wavelength away from the fundamental absorption edge. The maximum optical transparency (30 %) is observed for the film with composition  $x = 0.6$ , whereas others show optical transparency between 0-20% in the spectral range of 200-2500 nm. With increasing the composition of  $\text{Bi}_2\text{Te}_3$  ( $x = 0$  to 0.9) the absorption edge shifts towards lower wavelength region. For all the films and compositions the reflectance diverges between 10-60% in the spectral range of 200-2500 nm. The optical band gap has been found to be direct and allowed. The band gap increases from 0.62 to 0.82 with increase in composition from  $x = 0.1$  to 0.9. The value of extinction coefficient 'k' varies between 0.36 and 1.48, while refractive index 'n' varies between 1.48 and 7.64, for all the compositions.

#### ACKNOWLEDGEMENT

I would like to express my sincere gratitude to my esteemed Research Guide, Prof. Dr. P. H. Pawar, Prin. Dr. G. B. Shelke for his invaluable guidance, continuous support, and encouragement throughout the course of this research work.

#### REFERENCES

- [1] Ali, N., Zubair, et al (2021). A Study on Optoelectronic Properties of Copper Zinc Tin Sulfur Selenide: A Promising Thin Film Material for Next Generation Solar Technology. *Crystal Research and Technology*, 56(7). <https://doi.org/10.1002/crat.202000159>.
- [2] Dory, J., et al (2020). Ge-Sb-S-Se-Te amorphous chalcogenide thin films towards on-chip nonlinear photonic devices. *Scientific Reports*, 10(1). <https://doi.org/10.1038/s41598-020-67377-9>.
- [3] Furdyna, J. K., et al (2020). The ubiquitous nature of chalcogenides in science and technology. In Elsevier eBooks (p. 1). Elsevier BV. <https://doi.org/10.1016/b978-0-08-102687-8.00001-4>.
- [4] Ho, C. (2020). Ga<sub>2</sub>Se<sub>3</sub> Defect Semiconductors: The Study of Direct Band Edge and Optical Properties. *ACS Omega*, 5(29), 18527. <https://doi.org/10.1021/acsomega.0c02623>.
- [5] Mergen, Ö. B., et al (2020). Determination of Optical Band Gap Energies of CS/MWCNT Bio-nanocomposites by Tauc and ASF Methods. *Synthetic Metals*, 269, 116539. <https://doi.org/10.1016/j.synthmet.2020.116539>.
- [6] Gholipour, B., et al (2022). Roadmap on chalcogenide photonics. *Journal of Physics Photonics*, 5(1), 12501. <https://doi.org/10.1088/2515-7647/ac9a91>.
- [7] A. Kumar, P. Heera, P. Sharma, P. B. Barman and R. Sharma, *J. of Non-Crystalline Solids*, 358 (2012) 3223-3228.
- [8] S. Augustine, S. Ampili, J. Ku Kang and E. Mathai, *Materials Research Bulletin*, 40 (2005) 1314-1325.
- [9] A. Zimmer, N. Stein, H. Terryn and C. Boulanger, *J. of Physics and Chemistry of Solids*, 68 (2007) 1902-1907.
- [10] S. M. Patil, S. N. Gavale, R. K. Mane et al., *Arch. Phy. Res.*, 3(3) (2012) 245- 257.
- [11] A. Goswami, *Thin Film Fundamentals*, New Age International Pvt. Ltd., (2014) 442.
- [12] P. B. Barman and P. Sharma, *Glass Physics and Chemistry*, 39(3) (2013) 276-278.
- [13] K. Sharma, M. Lal and Goyal, *J. of Optoelectronics and Biomedical Materials*, 6 (2014) 27-34.